Scientific Research Publishing

World Journal of Mechanics, 2024, 14, 23-53
https://www.scirp.org/journal/wjm
ISSN Online: 2160-0503
ISSN Print: 2160-049X

Theory of Flexural Shear, Bending and Torsion for a Thin-Walled Beam of Open Section

David W. A. Rees, Abdelraouf M. Sami Alsheikh

College of Engineering and Design, Brunel University, Uxbridge, UK
Email: David.Rees@brunel.ac.uk, dralsheikh1948@gmail.com

How to cite this paper: Rees, D.W.A. and Alsheikh, A.M.S. (2024) Theory of Flexural Shear, Bending and Torsion for a Thin-Walled Beam of Open Section. *World Journal of Mechanics*, **14**, 23-53.
https://doi.org/10.4236/wjm.2024.143003

Received: November 10, 2023
Accepted: March 26, 2024
Published: March 29, 2024

Abstract

Aspects of the general Vlasov theory are examined separately as applied to a thin-walled channel section cantilever beam under free-end end loading. In particular, the flexural bending and shear that arise under transverse shear and axial torsional loading are each considered theoretically. These analyses involve the location of the shear centre at which transverse shear forces when applied do not produce torsion. This centre, when taken to be coincident with the centre of twist implies an equivalent reciprocal behaviour. That is, an axial torsion applied concentric with the shear centre will twist but not bend the beam. The respective bending and shear stress conversions are derived for each action applied to three aluminium alloy extruded channel sections mounted as cantilevers with a horizontal principal axis of symmetry. Bending and shear are considered more generally for other thin-walled sections when the transverse loading axes at the shear centre are not parallel to the section = s centroidal axes of principal second moments of area. The fixing at one end of the cantilever modifies the St Venant free angular twist and the free warping displacement. It is shown from the Wagner-Kappus torsion theory how the end constrained warping generates an axial stress distribution that varies with the length and across the cross-section for an axial torsion applied to the shear centre. It should be mentioned here for wider applications and validation of the Vlasov theory that attendant papers are to consider in detail bending and torsional loadings applied to other axes through each of the centroid and the web centre. Therein, both bending and twisting arise from transverse shear and axial torsion applied to each position being displaced from the shear centre. Here, the influence of the axis position upon the net axial and shear stress distributions is to be established. That is, the net axial stress from axial torsional loading is identified with the sum of axial stress due to bending and axial stress arising from constrained warping displace-

ments at the fixing. The net shear stress distribution overlays the distributions from axial torsion and that from flexural shear under transverse loading. Both arise when transverse forces are displaced from the shear centre.

Keywords

Thin Wall Theory, Cantilever Beam, Open Channel Section, Principal Axes, Flexure, Transverse Shear, Torsion, Shear Centre, Shear Flow, Warping, Fixed-End Constraint

1. Introduction

In a minor departure from the Vlasov theory [1], here the co-ordinates z refers to length while x and y lie in the cross section with their origin at the centroid. (Vlasov replaces z with x, and x with z). Many extruded beam cross-sections are symmetrical on either side of the vertical y-axis upon which the centroid will lie. Consequently, when the line of action of a vertical shear force is aligned with the y-axis of these sections, there will be no twisting effect. That is not to say, generally, that when the force passes through the centroid that longitudinal twisting is avoided. For a section that is not symmetrical about a vertical y-axis, as with the vertically mounted channel considered here, then the shear force must be displaced to pass through a point called the *shear centre* if the beam is not to twist [2] [3]. This ensures that the shear stress distribution over a section is statically equivalent to the applied shear force, *i.e.* the distribution has a zero moment about any point in the line of the shear force. It follows that twisting can be avoided in a non-uniform beam section when the transverse shear forces applied over the length lie on a longitudinal *flexural axis* that is the locus of the shear centres for all cross-sections. That locus is a straight line for a channel cross-section uniform in the length. The shear centre is a property of the section not generally coincident with the centroid [4]. The shear centre of a doubly or a multiply symmetric section does lie at the centroid and here the flexural axis is coincident with the centroidal axis. The shear centre of a singly symmetrical channel section lies on its x-axis of symmetry and the flexural axis will lie in the plane of symmetry. It is often obvious from inspection where the shear centre is located. It will lie at the intersection of the limbs in tee, angle and crucifix sections as this is the point of intersection between the force resultants of the shear stress distributions for those limbs.

In practice, transverse shear forces are not always applied concurrent with the shear centre E (see **Figure 1(a)**). Shear stresses due to torsion from the offset loading as well as flexural shear both appear (see **Figure 1(b)** and **Figure 1(c)**).

The static equivalence between **Figure 1(a)** and the sum of **Figure 1(b)** and **Figure 1(c)** enables the net shear stress to be found by adding the separate effects of pure flexural shear and pure torsion.

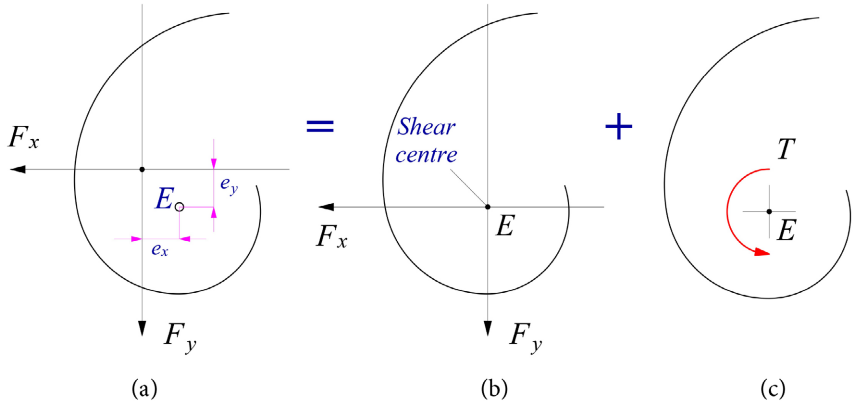

Figure 1. Superposition of pure flexural shear and torsion.

St Venant's theory [4] [5] provides the shear stress due to torsion for a thin-walled, open section when the beam ends that bear axial torsion are unconstrained. In the case of I, T and U sections it will be seen that the contribution to the net torque T from the individual, thin straight limbs (the web and the flanges) may be added by that theory. In what follows to find the shear stress across the thickness in **Figure 1(c)**, the applied torque arising from transverse perpendicular forces F_x and F_y acting at the centroid G is given as: $T = F_x e_y + F_y e_x$ where (e_x, e_y) are the co-ordinates of the shear centre E.

2. Shear Flow in Thin-Walled Sections

The following discussion illustrates how the shear flow distribution and the position of the shear centre may be found in the case of open thin-walled sections. Consider a beam with an open section of arbitrary shape. The wall thickness may vary but must remain thin compared to the other dimensions (see **Figure 2(a)**). Centroidal axes x and y pass through the centroid G for which the directions of the transverse shear forces F_x and F_y are aligned. If the cross-section is not to twist, both shear forces must act through the shear centre E which is displaced from G. Let F_x and F_y act at E in the negative x and y directions as shown, so that *positive hogging* moments M_x and M_y appear in the first quadrant of (x, y), In a beam with both ends supported the transverse point forces applied to the span and their accompanying bending moments will vary with beam length. Recall here, the construction of shear force and bending moment diagrams for these variations [6]. Within the plane of the thin wall cross-section there will be a component of shear stress τ_{zs} parallel to the mid-wall centre-line co-ordinate s, where the material is assumed to be concentrated, and one normal to this mid-line, τ_{zn} where n is perpendicular to s. Because τ_{zn} is zero at the free edges, its variation with t can be ignored. Also, τ_{zs} is assumed to be uniform between the edges of a thin section but will vary with the perimeter length s. Here a constant shear flow $q = t\tau_{zs}$ will account for variations in τ_{zs} with a varying t around the section in the positive s-direction shown. This applies to transverse shear force but note that shear stress due to torsion of an open tube varies linearly

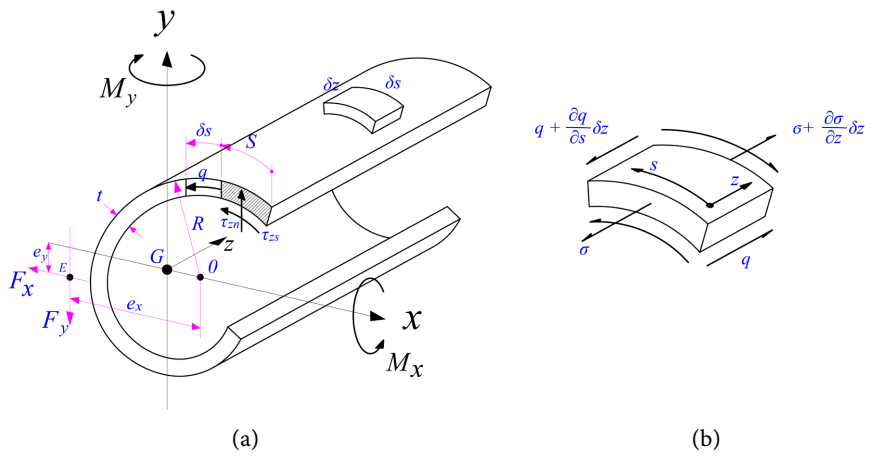

(a) (b)

Figure 2. Shear flow in a thin-walled open section.

through the thickness [6] where a zero average shear stress is referred to the mid centre line.

Acting in the z-direction there is a mid-line complementary shear flow, $q = t\tau_{sz}$ and a bending stress σ due to the bending moment. The variation in these actions across an element $\delta s \times \delta z$ of the wall is shown in **Figure 2(b)**. When any slight variation in t with δs is ignored, the equilibrium equation for the z-direction becomes

$$\left[\sigma+\left(\partial\sigma/\partial z\right)\delta z\right]\left(\delta s\times t\right)-\sigma\left(\delta s\times t\right)-\left[q+\left(\partial q/\partial s\right)\delta s\right]\delta z+q\delta z=0$$

This simplifies to the following equilibrium equation between q and σ when they increase with positive s and z:

$$\partial q/\partial s = t\,\partial\sigma/\partial z \tag{1}$$

Since both M_x and M_y are positive (hogging) moments within first quadrant (x, y) in **Figure 2(a)**, the longitudinal bending stress is

$$\sigma = M_x y/I_x + M_y x/I_y \tag{2}$$

Substituting Equation (2) into Equation (1) and integrating for the shear flow q

$$q=\left(1/I_x\right)\int\left(\mathrm{d}M_x/\mathrm{d}z\right)\left(yt\mathrm{d}s\right)+\left(1/I_y\right)\int\left(\mathrm{d}M_y/\mathrm{d}z\right)\left(xt\mathrm{d}s\right) \tag{3}$$

The hogging moments for any section at a distance z from the origin in **Figure 2(a)** are $M_x = F_y z$ and $M_y = F_x z$. Hence the transverse shear forces follow:

$$F_y=\mathrm{d}M_x/\mathrm{d}z \quad \text{and} \quad F_x=\mathrm{d}M_y/\mathrm{d}z \tag{4a, b}$$

That is, F_x and F_y are positive shear forces associated with the hogging moments. Equations (4a, b) will connect the forces to the moments for any section distance z along the beam. Substituting Equations (4a, b) into Equation (3) gives,

$$q=\left(F_y/I_x\right)D_x+\left(F_x/I_y\right)D_y \tag{5}$$

where $D_x=\int yt\mathrm{d}s$ and $D_y=\int xt\mathrm{d}s$ are the respective first moments of the incremental area $t\,\delta s$ about the x and y axes in **Figure 2(a)**. Equation (5) will give a

positive q for the negative F_x and F_y directions shown and with s measured anti-clockwise from the free surface.

Equation (5) is not restricted to positive forces. The sign of q will indicate its true direction relative to the chosen direction for s.

2.1. Principal Axes

This far we have specified that x and y are centroidal axes lying parallel to the shear forces F_x and F_y. Equation (5) applies when x and y coincide with the principal axes for the section, *i.e.* when I_x and I_y are the principal second moments of area for the asymmetric section, as shown in **Figure 3(a)**.

In contrast, for the non-symmetric cross-section in **Figure 3(b)**, shear forces F_x and F_y, applied at E, are not aligned with its principal directions u and v. Equations (2) and (5) become

$$\sigma = M'_x y/I_x + M'_y x/I_x \tag{6a}$$

$$q = \left(F'_y/I_x\right)D_x + \left(F'_x/I_y\right)D_y \tag{6b}$$

where equivalent shear force components F'_x and F'_y may be derived from the equivalent moments M'_x and M'_y employed with the asymmetric bending of beams [6]. Equivalent moments refer co-ordinates x, y to the centroid G for which non-principal second moments I_x, I_y and I_{xy} apply. These equivalent quantities offset the need to calculate principal second moments for axes u and v and their respective orientations [7].

$$M'_x = \left[M_x - M_y\left(I_{xy}/I_y\right)\right]\Big/\left[1-\left(I_{xy}^2/I_xI_y\right)\right] \tag{7a}$$

$$M'_y = \left[M_y - M_x\left(I_{xy}/I_x\right)\right]\Big/\left[1-\left(I_{xy}^2/I_xI_y\right)\right] \tag{7b}$$

Applying the derivative relationships between F and M in Equations (4a, b) to Equations ((7a), (7b)) give:

$$F'_y = \left[F_y - F_x\left(I_{xy}/I_y\right)\right]\Big/\left[1-\left(I_{xy}^2/I_xI_y\right)\right] \tag{8a}$$

$$F'_x = \left[F_x - F_y\left(I_{xy}/I_x\right)\right]\Big/\left[1-\left(I_{xy}^2/I_xI_y\right)\right] \tag{8b}$$

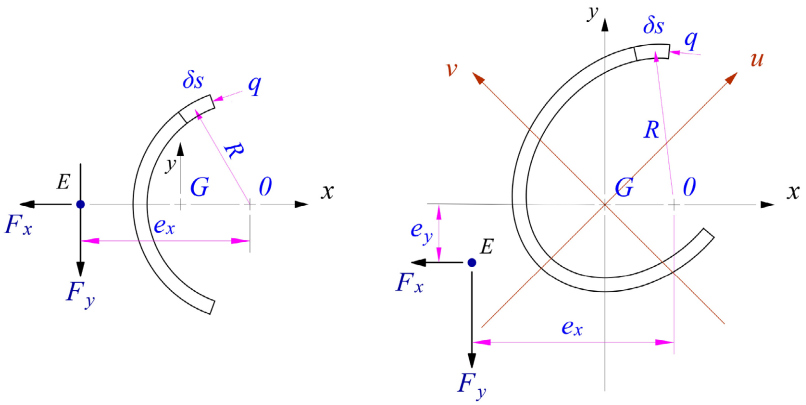

Figure 3. Principal axes (a) coincident and (b) not coincident with shear force directions.

2.2. Shear Centre

To find the position of the shear centre E in Figure 3(b), the following principle applies to any point O in the section: the moment due to shear flow q will be equivalent to the resultant moment produced by shear forces F_x and F_y acting at E. For example, taking moments about a point O on the x-axis in Figure 3(b), the resultant moment is

$$F_y e_x - F_x e_y = \int qR\mathrm{d}s \tag{9a}$$

where R is the perpendicular distance of q from O. Equation (9a) alone cannot locate the shear centre position E (e_x, e_y) for an asymmetric section. However, the moment due to one of the forces in Equation (9a) can be eliminated when O is chosen to lie along either force line. This method is adopted to find the shear centre for a thin section that is symmetrical about either axis x or y. For example, in Figure 3(a) we need only apply a single vertical force F_y at E to find the position e_x of E from O. That is, for Figure 3(a), the applied force F_x is removed, modifying Equation (9a) to

$$F_y e_x = \int q'R\mathrm{d}s \tag{9b}$$

where q' is the shear flow under F_y acting alone. Equations ((9a), (b)) may then be solved for e_x and e_y.

2.3. Singly Symmetrical Sections

Shear flow analysis is simplified when a section is symmetric about either of its centroidal axes x or y. This means that x and y are principal axes and that both the centroid G and the shear centre E will lie along the axis of symmetry (the x-axis in Figure 3(a)). In the case of a symmetrical section under a single shear force F_x (or F_y), one or other term is omitted from Equation (5). For example, if in Figure 3(a), F_x is absent then the shear flow equation becomes

$$q_x = \left(F_y / I_x\right) D_x \tag{10a}$$

With x the symmetry axis, the shear centre E (e_x, 0) is found from taking moments at O:

$$F_y e_x = \int qR\mathrm{d}s \tag{10b}$$

Here Equation (10b) applies irrespective of whether F_x is present or not.

2.4. Summary of Flexural Shear

If the beam of thin-walled section is not to twist under transverse force components F_x and F_y they are to be applied to the *shear centre* of that section whether it be open or closed. The shear centre will lie along or at the intersection between the section's axes of symmetry where they exist. The shear flow q, as found from Equation (5), will be seen to vary with the dimension s taken around the section perimeter. The origin for s, where $q = 0$, is taken to lie at a free surface in an open section and, where it exists, at the intersection between the thin wall and an

axis of symmetry for a closed section. The analysis proceeds with thin open sections generally and axially-symmetric channel sections in particular.

3. Shear Flow in Thin-Walled Open Sections

An interesting feature of shear stress arising from transverse shear forces applied to beams is the concept of shear flow within open cross-sections having thin walls. It has been seen generally that shear flow is the product of the shear stress and the wall thickness $q = \tau t$. In Equation (10a), under a single transverse force F_y, the shear flow q_x is found from

$$q_x = F_y D_x / I_x \tag{11a}$$

where D_x and I_x are, respectively, the first and second moment of the section area about the x-axis. Both moments of area derive from integrating an element of the wall area $t\delta s$ about the x-axis:

$$D_x = \int_s yt\mathrm{d}s \quad \text{and} \quad I_x = \int_s y^2 t\mathrm{d}s \tag{11b, c}$$

Within Equations (11b, c), the integration for I_x must extend over the whole cross section but that for D_x applies only to the area that contains s. If the beam is not to twist one must identify F_y with a vertical force applied at the *shear centre* of an open section. Here the shear centre will lie along or at the intersection between the section's axes of symmetry. If the shear centre position is not obvious it will need to be calculated as in the examples to follows. The shear flow q, as found from Equation (11a), will be seen to vary with the dimension s taken around the section perimeter. Conveniently, the origin for s is taken to lie at a free surface in an open section where $q_x = 0$.

Where a second, horizontal shear force F_x acts at the shear centre Equation (5) shows that the respective shear flows may be added from the separate applications of forces F_x and F_y. Adopting this *principle of superposition*, the net shear flow is given in full:

$$q = \left(F_y D_x / I_x\right) + \left(F_x D_y / I_y\right) \tag{12a}$$

where in addition to Equations (11b, c) and by analogy

$$D_y = \int_s xt\mathrm{d}s \quad \text{and} \quad I_y = \int_s x^2 t\mathrm{d}s \tag{12b, c}$$

The derivation of Equations (11a) and (12a) assumes that x and y are the section's principal axes and that, in the present convention, shear forces F_x and F_y are applied in opposite directions to positive x and y.

3.1. Open Channel

In the channel section shown in **Figure 4(a)**. The vertical shear force is placed at the shear centre E, whose position e_x is to be found along the x-axis of symmetry. Also, to be established here are expressions for the shear flow q_x-distributions around the section's web and flanges, shown in **Figure 4(b)**.

Because x is a symmetry axis, it will contain both G and E but they are not coincident for a singly symmetric channel section. Here centroidal axes x and y

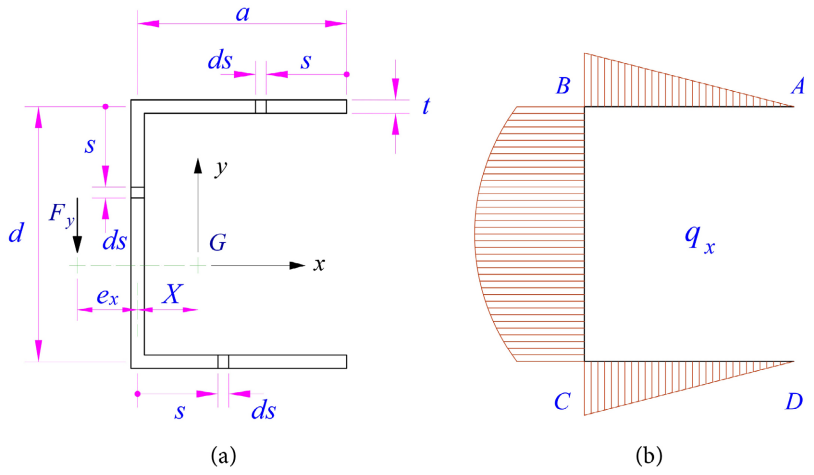

Figure 4. Shear flow in a uniformly thin channel with vertical force at E.

at G are the section's *principal axes* and therefore Equation (11a) will provide the shear flow directly. The position X' of its centroid G is found from taking first moments of the three rectangular areas about the web's vertical edge BC:

$$t(dt/2)+2at(a/2)=(2a+d)tX'$$

from which

$$X'/a=(a/d)/\left[1+2(a/d)\right] \tag{13a}$$

which is an acceptable approximation when $t \ll a$ for a thin wall. With the origin of the axes x and y at the centroid G, as shown, I_x is the only second moment of area required:

$$I_x=2\left[\left(at^3\right)/12+at(d/2)^2\right]+td^3/12\approx\left(td^2/2\right)(a+d/6) \tag{13b}$$

Taking the origin for s at A, the shear flow in the top flange AB becomes:

$$q_{AB}=\left(F_y/I_x\right)\int_s ytds=\left(F_y/I_x\right)\int_s(d/2)tds=F_ys/\left[d(a+d/6)\right] \tag{14}$$

Equation (14) gives a linear distribution having its maximum at B, *i.e.* q_B for $s = a$ (as shown in **Figure 4(b)**). The q_B-value reappears in the shear flow integral for web BC as follows:

$$q_{BC}=\left(F_y/I_x\right)\int_s ytds+q_B=\left(F_y/I_x\right)\int_s(d/2-s)tds+F_ya/\left[d(a+d/6)\right] \tag{15a}$$

where the origin for s is at B. Integrating Equation (15a) and substitution for I_x gives:

$$q_{BC}=\left(F_yt/I_x\right)\int_s ytds+q_B=\left(F_y/I_x\right)\int_s(d/2-s)tds+F_ya/\left[d(a+d/6)\right] \tag{15b}$$

Equation (15b) describes the parabolic distribution shown in **Figure 4(b)**, this revealing that the maximum shear flow occurs at the neutral x-axis ($s = d/2$):

$$q_{max}=F_y(a+d/4)/(a+d/4)=3F_y(1+4a/d)/2d(1+6a/d) \tag{15c}$$

Equation (15c) provides a maximum shear stress $\tau_{max} = q_{max}/t$, which is identical to that which would be found at the web-centre for a uniform I-beam with

flange lengths a and web depth d. However, the corresponding shear flow analyses must refer to the condition that F_y is applied at the shear centre E (see Figure 4(a)). While E coincides with the centroid for an I-section, it lies outside the channel section, distance e from the web as shown.

The requirement that F_y does not twist the section is met when the corresponding torque applied to the section $T = F_y e_x$ is the resultant of the net torque due to the q distributions in each limb. Such a *static equivalence* condition must apply to *any* point around the perimeter. Hence by taking the corner point C, for example, only the shear flow in AB is influential in providing the static equivalence equation. That is, taking moments at C:

$$\Sigma T_C = F_y e_x - d\int_0^a q_{AB}\mathrm{d}s = 0 \tag{16a}$$

and substituting q_{AB} from Equation (14), e_x/a is found from Equation (16a) as:

$$F_y e_x = d\int_0^a q_{AB}\mathrm{d}s$$

$$\therefore e_x/a = 3(a/d)/(1+6a/d) \tag{16b}$$

If F_y is not applied at E then shear stress arises from both shear force and torsion. Such a combination arises when F_y acts vertically at the centroid G or along the web (say).

Conveniently, shear and torsion may be separated and superimposed to provide the net effect upon shear stress, twist and warping. In this paper the torsional effects are considered and in a second paper [8] offset shear force effects are examined for channel sections in particular. The example given above shows that the shear flow must be considered initially in order to locate the required position of the shear centre to enable the superposition mentioned. A further example follows below to illustrate how the shear flow distribution provides the location of E in a section with curvature.

3.2. Semi-Circular Shell

Here it is required to determine the shear flow distribution and the position of the shear centre for a thin-walled semi-circular section. Transverse loading is applied through the shear centre E by shear forces F_x and F_y lying parallel to the principal axes x and y as shown in Figure 5(a).

Firstly, the position $\bar{X}$ of the centroid G is found by taking the first moments of area about the Y-axis shown. Let s and δs subtend angles θ and $\delta\theta$ at O in Figure 5(a). The first moment of area theorem is applied as follows with $\delta s = R\delta\theta$

$$A\bar{X} = \int x\mathrm{d}A$$

$$(\pi Rt)\bar{X} = \int_0^\pi (R\sin\theta)Rt\mathrm{d}\theta$$

$$\bar{X} = (R/\pi)\int_0^\pi \sin\theta\mathrm{d}\theta = 2R/\pi \tag{17a}$$

Both I_x and I_y are required in this example:

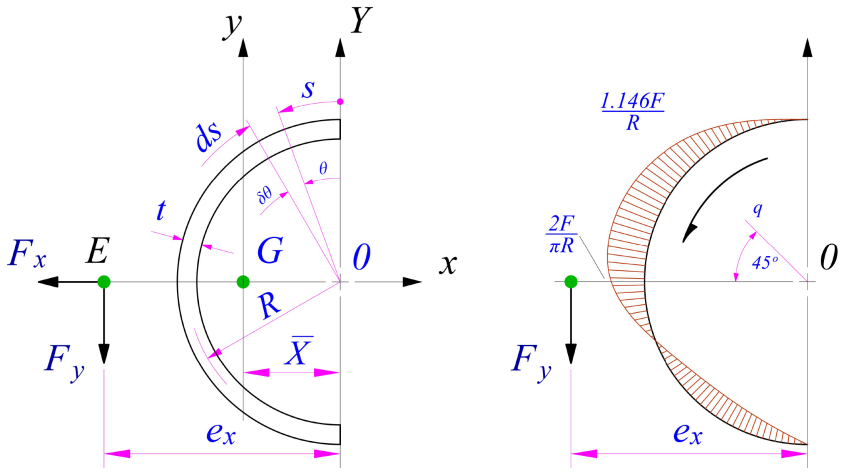

Figure 5. Semi-circular section under transverse shear forces applied at E.

$$I_X = \int y^2 \mathrm{d}A = 2\int_0^{\frac{\pi}{2}} (R\cos\theta)^2 (Rt\mathrm{d}\theta) = \pi R^3 t/2$$

$$I_Y = \int x^2 \mathrm{d}A = 2\int_0^{\frac{\pi}{2}} (R\sin\theta)^2 (Rt\mathrm{d}\theta) = \pi R^3 t/2 \tag{17b}$$

and, from Equation (1.17a), within the parallel axis theorem:

$$I_y = I_Y - A\bar{X}^2$$

$$I_y = \pi R^3 t/2 - (\pi Rt)(2R/\pi)^2 = R^3 t(\pi/2 - 4/\pi) \tag{17c}$$

The first moment integrals within Equation (5) are

$$D_x = \int ty\mathrm{d}s = \int_0^\theta t(R\cos\theta)(R\mathrm{d}\theta) = \int_0^\theta R^2 t\cos\theta \mathrm{d}\theta = \left[R^2 t\sin\theta\right]_0^\theta$$

$$D_x = R^2 t\sin\theta \tag{18a}$$

$$D_y = \int tx\mathrm{d}s = \int_0^\theta t(2R/\pi - R\sin\theta)(R\mathrm{d}\theta) = \left[2tR^2\theta/\pi + R^2 t\cos\theta\right]_0^\theta$$

$$D_y = R^2 t(2\theta/\pi + \cos\theta - 1) \tag{18b}$$

Here, both F_x and F_y are reckoned positive as acting in the negative x- and y-directions.

Substituting Equations ((17b), (18c)) and ((18a), (18b)) into Equation (5) results in the following expression of q in terms of θ:

$$q = (2F_y/\pi R)\sin\theta + 2\pi F_x(2\theta/\pi + \cos\theta - 1)/R(\pi^2 - 8) \tag{19a}$$

which is positive for the direction of s shown. When $F_x = F_y = F$, the shear flow varies around the perimeter as in Figure 5(b). This shear flow distribution is statically equivalent to the two applied shear forces, provided that they act through the shear centre E. In this case E will lie along the x-axis, say distance e_x from O. By taking moments about O, it is only necessary to consider moment equivalence between F_y and the component of shear flow due to F_y. That is from Equation (19a):

$$q = \left(2F_y/\pi R\right)\sin\theta \tag{19b}$$

Applying the integral in Equation (10b) to the perimeter path

$$F_y e_x = \int qR\mathrm{d}s = \int \left(2F_y/\pi R\right) R\sin\theta \mathrm{d}s$$

Substituting $\delta s = R\delta\theta$, into Equation (19b), the integral is evaluated for e_x within limits: $0 \le \theta \le \pi$ (rad):

$$F_y e_x = R^2 \int_0^\pi q\mathrm{d}\theta = 2R\left(F_y/\pi\right)\int_0^\pi \sin\theta \mathrm{d}\theta = -2R\left(F_y/\pi\right)\left[\cos\theta\right]_0^\pi = 4RF_y/\pi$$

$$\therefore e_x = 4R/\pi \tag{19c}$$

Equation (19c) locates the position of the shear centre horizontally from the centre O of the semi-circle, as shown in **Figure 5(a)** and **Figure 5(b)**.

4. Wagner-Kappus Torsion of Thin-Walled, Open Sections

The forgoing examples provide the analyses required for locating the position of the shear centre for a thin-walled, open cross-section beam subjected to transverse forces. Knowing the position of the shear centre is equally important for when torsion is applied to an open section cantilever beam about a longitudinal axis.

4.1. Centre of Twist

Of all the axes about which torsion may be applied to the section one above all others underlies the analyses of the deformation that torsion produces. Consider a thin-walled open tube subjected to an axial torque about a longitudinal *z*–axis passing through the section's *centre of twist*. The latter exists as a point in the cross-section when there is no resultant torque about other longitudinal axes lying within the open-section's plane in **Figure 6(a)**. The centre of twist will not coincide with the centroid of the cross-section in general. However, the analysis of an open tube is simplified by knowing that the centre of twist coincides with the *shear centre* for the section [5]. It has been seen that the shear centre refers to that point in the section through which a transverse shear force must pass if it

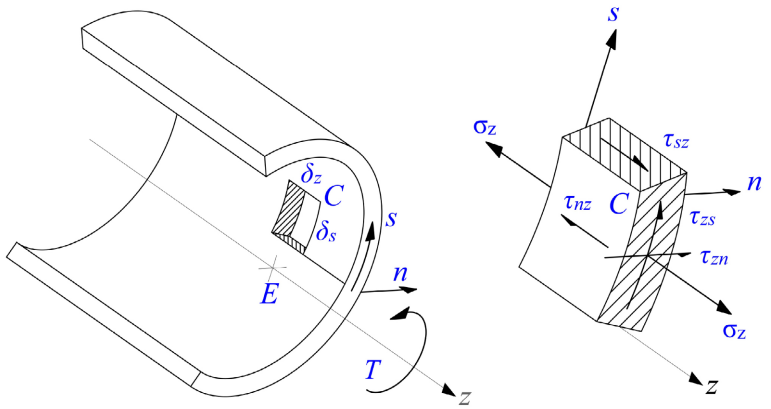

(a) (b)

Figure 6. Element of a thin-walled open tube under torsion.

is to bend but not twist the beam. Moreover, a torque must be applied about a longitudinal axis through the centre of twist if it is to twist and not to bend the beam. By deduction, taking a reciprocal relationship to apply between these two centres, for shear and torsion, has assumed their coincidence [9]. *Note*: Depending upon the cross-section, a more rigorous proof, based upon minimal strain energy arising from each of the loadings applied separately to the shear centre [10] may not predict the coincidence assumed.

4.2. Restrained Warping

The St Venant torsion theory cannot be applied to a beam with one end fixed due to the constraint that the end-fixing imposes. Let axial co-ordinate axis z pass through E. Section co-ordinate s lies along the mid-wall perimeter and co-ordinate n is aligned with the direction of the normal to the mid-wall (see **Figure 6(a)** and **Figure 6(b)**).

In **Figure 6(b)** the shear stresses τ_{nz} and τ_{sz} $(=\tau_{zs})$ within an element $\delta s \times \delta z$ of the wall are shown with their complementary action. The elemental length δs subtends an area δA_E at E:

$$\delta A_E = (1/2) R_t \delta s \tag{20}$$

Restraining warping in the z-direction will introduce an axial stress σ_z as shown. Consider a point C lying upon the median co-ordinate s. If we draw the tangent to s at this point then normal and tangential radii, R_n and R_t for C respectively, are centred at E, shown in **Figure 7(a)**.

4.3. Unconstrained Warping

When there are no constraints to twist, the tube will warp freely in its length. Let the tube wall twist by the small amount $\delta\theta$ at E so that point C moves to C′ in **Figure 7(b)**. The tangential and normal components of this displacement are: $R_t \delta\theta$ and $R_n \delta\theta$ respectively. Two warping displacements of C, δw_s and δw_n, are aligned with the length. They are found from the shear distortion of the element in two planes, $s-z$ and $n-z$, as shown in **Figure 8(a)** and **Figure 8(b)**.

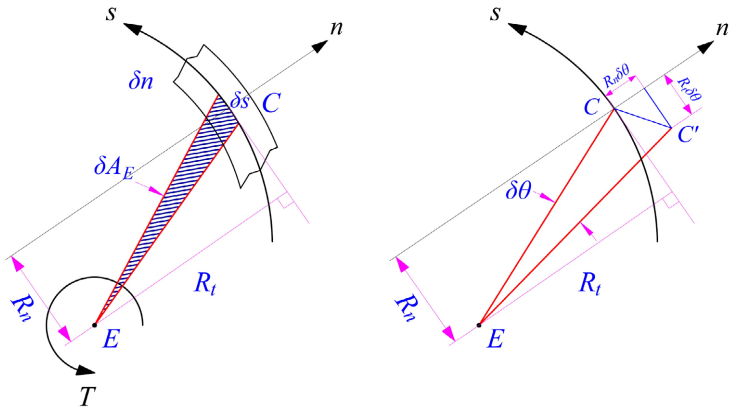

(a) (b)

Figure 7. Normal and tangential radii R_n and R_t to median co-ordinate s.

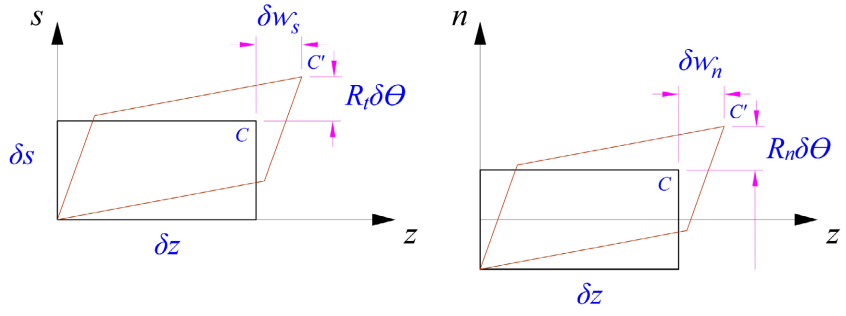

(a) (b)

Figure 8. Shear distortion to the wall of an open tube under torsion.

The primary warping displacement, w_s in **Figure 8(a)**, occurs in the $s-z$ plane and is constant across the wall. The corner C will warp by an amount δw_s in the direction of z. C also displaces tangentially by the amount $R_t\delta\theta$. The shear strain γ_{sz} in the $s-z$ plane is the sum of these two shear angles

$$\gamma_{sz} = \delta w_s/\delta s + R_t\,\delta\theta/\delta z \tag{21a}$$

Secondary warping w_n, occurs in the $n-z$ plane and varies through the wall in the manner of **Figure 8(b)**. The mid-wall shear strain is given as

$$\gamma_{nz} = 1/2\left(\delta w_n/\delta n\right) + R_n\,\delta\theta/\delta z \tag{21b}$$

Under pure torsion the shear stress in the wall of a tube varies linearly through the thickness to obtain maximum values at the inner and outer edges. Hence, the two shear stresses associated with each shear strain in Equations ((21a), (b)) are: $\tau_{sz} = G\gamma_{sz}$ and $\tau_{nz} = G\gamma_{nz}$. These are to equal zero along the mid-line from which the two incremental warping displacements follow:

$$\delta w_s = -R_t\left(\delta\theta/\delta z\right)\delta s \text{ and } \delta w_n = -2R_n\left(\delta\theta/\delta z\right)\delta n \tag{22a, b}$$

Now from Equation (20) $R_t\delta s = 2\delta A_E$ where R_t will depend upon s but R_n is taken to be independent of n. Hence the *primary* and *secondary* warping displacements [11] become

$$w_s = -\left(\delta\theta/\delta z\right)\int_0^s R_t\mathrm{d}s = -2A_E\,\delta\theta/\delta z \tag{23a}$$

$$w_n = -2R_n n\,\delta\theta/\delta z \tag{23b}$$

where $\delta\theta/\delta z = T/(GJ)$ and A_E is the area swept between E, the datum $s = 0$ (where $w = 0$) and the perimeter length s (see **Figure 9(a)**). The total warping displacements at point (s, n) is found from Equations ((23a), (23b)) as $w = w_s + w_n$. In fact, an unconstrained secondary warping w_n is usually negligible compared with primary warping w_s but where the former matters it is considered separately in §4.7. The analysis proceeds with primary warping but note that A_E in Equation (23a) will be incorrect by an amount A_E' when the datum $s = 0$ does not coincide with a point of zero warping displacement (see **Figure 9(b)**). However, Equation (23a) provides the relative displacements between points correctly. When Equation (23a) is applied between free surface points, the primary warping displacement w_s will be found to be independent of the position of

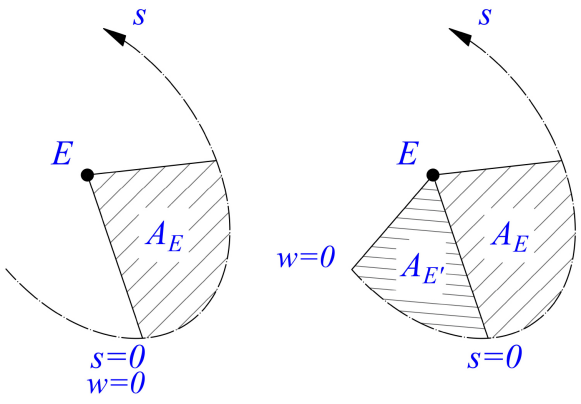

Figure 9. Areas A_E and A_E' enclosed between the shear centre E and the mean wall perimeter.

E, which is normally coincident with the centre of twist, *i.e.* at the centre of rotation [12].

4.4. Constrained Primary Warping

It may not be obvious where a point of zero warping lies and so by taking an arbitrary origin for s, where there is a warping displacement, the swept volume required is overestimated by an amount A_E' (see **Figure 9(b)**). To correct this, it is known that axial stress induced from constraining a primary warping displacement has no resultant force. This condition gives

$$\int_0^s \sigma_z t \mathrm{d}s = 0 \tag{24a}$$

The strain ε_z, arising from the uniaxial elastic stress σ_z, obeys Hooke's law:

$$\sigma_z = E\varepsilon_z = E\left(\partial w_s / \partial z\right) \tag{24b}$$

Substituting Equation (23a) into Equation (24b) gives,

$$\sigma_z = -2A_E E \,\mathrm{d}^2\theta / \mathrm{d}z^2 \tag{24c}$$

Now θ is independent of s, varying only with z and, therefore, from Equations ((24a), (24c)),

$$-E\left(\mathrm{d}^2\theta/\mathrm{d}z^2\right)\int_0^s 2A_E t \mathrm{d}s = 0$$

$$\therefore \int_0^s 2A_E t \mathrm{d}s = 0 \tag{25a}$$

Let $A_{os} = A_E + A_E'$ be the total area swept from $s = 0$ in **Figure 9(b)**. Equation (25a) becomes

$$\int_0^s 2A_{os} t \mathrm{d}s - 2A_{E'}\int_0^s t \mathrm{d}s = 0 \tag{25b}$$

Writing $\bar{y} = 2A_{E'}$ and $y = 2A_{os}$ and taking t as a constant, Equation (25b) gives $\bar{y}$ as

$$\bar{y} = \int y \mathrm{d}s \Big/ \int \mathrm{d}s \tag{25c}$$

Equation (25c) can be interpreted in the manner of Figure 10 below. This shows that $\bar{y}$ is the height of a rectangle with the same area as that area enclosed between y and the perimeter length s.

Hence in Equation (25a),

$$2A_E = 2A_{os} - 2A_{E'} = y - \bar{y} \tag{26}$$

Figure 11(a) and Figure 11(b) show the two planes, $s - z$ and $n - z$, within Figure 6(b), in which the axial and shear stresses are allowed to vary with δs in the manner shown.

The horizontal equilibrium equation for the element $\delta s \times \delta z$ in Figure 11(a), becomes

$$\left(\sigma_z + \left(\partial\sigma_z/\partial z\right)\delta z\right)t\delta s + \left(\tau_{sz} + \left(\partial\tau_{sz}/\partial s\right)\delta s\right)t\delta z = \sigma_z t\delta s + \tau_{sz}t\delta z$$

which reduces to

$$\left(\partial\sigma_z/\partial z\right) + \left(\partial\tau_{sz}/\partial s\right) = 0 \tag{27a}$$

The horizontal equilibrium equation for the element $\delta n \times \delta z$ in Figure 11(b) becomes

$$\left(\sigma_z + \left(\partial\sigma_z/\partial z\right)\delta z\right)t\delta n + \left(\tau_{nz} + \left(\partial\tau_{nz}/\partial n\right)\delta n\right)t\delta z = \sigma_z t\delta n + \tau_{nz}t\delta z$$

which gives

$$\left(\partial\sigma_z/\partial z\right) + \left(\partial\tau_{nz}/\partial n\right) = 0 \tag{27b}$$

Equation (27b) is used later in §4.7 for a secondary warping analysis. The primary warping analysis begins with wall shear flow q in the plane of the cross-section. Here q is associated with a constant shear stress τ_{sz} in the wall which follows from Equation (27a) as

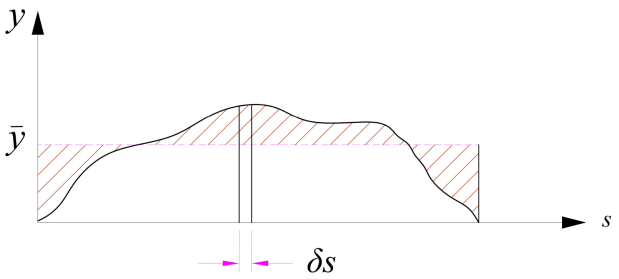

Figure 10. Graph of $y = 2A_{os}$ versus s showing $\bar{y}$.

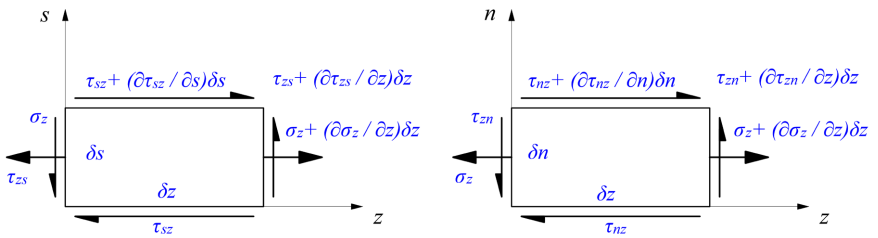

Figure 11. Stress variations across plane elements (a) $\delta s \times \delta z$, (b) $\delta n \times \delta z$.

$$q = t\tau_{sz} = -\int\left(\partial\sigma_z/\partial z\right)t\mathrm{d}s \tag{28a}$$

Substituting Equation (24c) into Equation (28a),

$$q = E\left(\mathrm{d}^3\theta/\mathrm{d}z^3\right)\int 2A_E t\mathrm{d}s \tag{28b}$$

The *Wagner-Kappus torque* [5] follows from the shear flow q as

$$T_w = \int_c qR_t\mathrm{d}s = E\left(\mathrm{d}^3\theta/\mathrm{d}z^3\right)\int_c R_t\left(\int_0^s 2A_E t\mathrm{d}s\right)\mathrm{d}s \tag{29a}$$

where $s = c$ is the full length along the mid-wall perimeter co-ordinate s. The following substitutions are made when integrating Equation (29a) by parts ($\int u\mathrm{d}v = uv - \int v\mathrm{d}u$) in combination with Equation (20):

$$T_w = \int_0^s u\mathrm{d}v$$

where,

$$u = \int_0^s 2A_E t\mathrm{d}s \text{ and } \mathrm{d}v = R_t\mathrm{d}s = 2\mathrm{d}A_E$$

when T_w follows:

$$T_w = E\left(\mathrm{d}^3\theta/\mathrm{d}z^3\right)\left[2A_E\int_c 2A_E t\mathrm{d}s - \int_c\left(2A_E\right)^2 t\mathrm{d}s\right] \tag{29b}$$

For a tube of constant thickness Equation (26) shows that $2A_E$ can be identified with the ordinate $y - \breve{y}$ in **Figure 10**. Hence, the first integral in Equation (29b) becomes zero, *i.e.* the nil sum of the areas lying above and below $\breve{y}$ as shown. Equation (29b) reduces to

$$T_w = -E\left(\mathrm{d}^3\theta/\mathrm{d}z^3\right)\int_c\left(2A_E\right)^2 t\mathrm{d}s = -E\Gamma_1\left(\mathrm{d}^3\theta/\mathrm{d}z^3\right) \tag{29c, d}$$

The integral term in Equation (29c) is a property of the section known as the *primary warping constant* Γ_1 (for torsion and bending) [13]. This constant may be found as follows:

$$\begin{aligned}\Gamma_1 &= \int\left(2A_E\right)^2 t\mathrm{d}s = \int\left(y-\breve{y}\right)^2 t\mathrm{d}s\\ &= \int y^2 t\mathrm{d}s - 2\breve{y}\int yt\mathrm{d}s + \int\breve{y}^2 t\mathrm{d}s\end{aligned} \tag{30a}$$

Substituting from Equation (25c): $\int yt\mathrm{d}s = \breve{y}\int t\mathrm{d}s$, defines Γ_1:

$$\Gamma_1 = \int y^2 t\mathrm{d}s - \int\breve{y}^2 t\mathrm{d}s \tag{30b}$$

If t is constant in Equation (30b) this simplifies to

$$\Gamma_1 = t\left(\int y^2\mathrm{d}s - \breve{y}^2\int\mathrm{d}s\right) \tag{30c}$$

in which the first term to be integrated is the square of the ordinate in **Figure 10** and the second integral is the perimeter length.

4.5. Twist Rate and Stiffness

The total torque is the sum of the St Venant and Wagner and torques $T = T_v + T_w$. The former follows as $T_v = GJ(\delta\theta/\delta z)$, where J for an open section, composed of thin rectangles breadth b and thickness t, is given as $J = \sum bt^3/3$. Adding T_w from Equation (29d)

$$T = GJ\,\mathrm{d}\theta/\mathrm{d}z - E\Gamma_1\,\mathrm{d}^3\theta/\mathrm{d}z^3 \tag{31}$$

The solution of Equation (31) provides the rate of twist, equal and opposite at the ends, where $z = 0$ and $z = L$ [14]:

$$\mathrm{d}\theta/\mathrm{d}z = \left(T/GJ\right)\left[1 - \cosh\mu\left(L - z\right)/\cosh\left(\mu L\right)\right] \tag{32a}$$

where $\mu = \sqrt{GJ/\left(E\Gamma_1\right)}$. Equation (32a) shows how the twist rate varies with length z in a tube constrained at one end. Integrating Equation (32a) and substituting $z = L$ gives the constrained angular twist at the free end:

$$\theta = \left(TL/GJ\right)\left[1 - \left(\mu L\right)^{-1}\tanh\mu L\right]$$

$$\theta = \left(T/\mu GJ\right)\left[\left(\mu L - 1\right) + \left(\mu L + 1\right)\exp\left(-2\mu L\right)\right]/\left[1 + \exp\left(-2\mu L\right)\right] \tag{32b}$$

from which the constrained beam's free-end "torsional stiffness" is

$$T/\theta = \mu GJ\left[1 + \exp\left(-2\mu L\right)\right]/\left[\left(\mu L - 1\right) + \left(\mu L + 1\right)\exp\left(-2\mu L\right)\right] \tag{32c}$$

Equation (32c) provides the amount by which the free St Venant's torsional stiffness $T/\theta = JG/L$ for the unconstrained tube is increased by fixing one end. From Equations (29d) and (32a), the Wagner torque is written as

$$T_w = -E\Gamma_1\left(\mathrm{d}^3\theta/\mathrm{d}z^3\right)$$

$$T_w = T\cosh\mu\left(L - z\right)/\cosh\left(\mu L\right) \tag{33a}$$

in which Equation (32a) has provided the third derivative as:

$$\mathrm{d}^3\theta/\mathrm{d}z^3 = -\left[\left(T\mu^2/GJ\right)\cosh\mu\left(L - z\right)\right]/\cosh\mu L \tag{33b}$$

Equation (33a) shows that at the fixed-end of the cantilever beam, where $z = 0$, $T_w = T$, *i.e.* all the torque is due to "bending" [5]. At the free end ($z = L$) T_w diminishes to $T/\cosh\mu L$, *i.e.* a bending contribution remains.

4.6. Axial Stress

With the warping constraint at the fixed-end, the axial stress is given from Equations (24c) and (32a) as

$$\sigma_z = -2A_E E\,\mathrm{d}^2\theta/\mathrm{d}z^2 = -2A_E\mu E \times T\mu\sinh\mu\left(L - z\right)/\cosh\mu L$$

$$\sigma_z = -\left(2A_E T/\mu\Gamma_1\right)\sinh\mu\left(L - z\right)/\cosh\mu L \tag{34a}$$

Hence σ_z is zero at the free end and attains a maximum at the fixed end. Using Equations (23a) and (26), the "free" primary warping displacement w_o is given as:

$$w_o = -2A_E\left(\delta\theta/\delta z\right) = -2A_E T/GJ = -\left(y - \breve{y}\right)T/GJ$$

Hence the coefficient in Equation (34a) appears in terms of w_o as

$$\therefore 2A_E T/\mu\Gamma_1 = -w_o GJ/\mu\Gamma_1 = -\mu E w_o \tag{34b}$$

Combining Equations ((24a), (24b)), it is seen how the axial stress is simplified:

$$\sigma_z = \mu E w_o\sinh\mu\left(L - z\right)/\cosh\left(\mu L\right) \tag{34c}$$

which shows that σ_z is proportional to w_o for a given position z in the length. Equation (24b) gives the constrained warping displacement at position $0 < z < L$,

$$w = (1/E)\int_0^z \sigma_z \mathrm{d}z \tag{35a}$$

Substituting Equation (34c) into (35a) and integrating,

$$w = \left[\mu w_o / \cosh(\mu L)\right]\int_0^z \sinh\left[\mu(L-z)\right]\mathrm{d}z$$

$$w = w_o\left[1-\cosh\mu(L-z)\right]/\cosh(\mu L) \tag{35b}$$

Equation (35b) shows that free warping displacement w_o exists partially at the free end ($z = L$) and is eliminated at the fixed end ($z = 0$). The problem of constrained warping in closed tubes is more complex than in thin-walled open tubes and sections, largely due to the uncertainty of an origin of s [15].

However, for doubly symmetric closed tubes, Equations (34c) and (35b) still apply. The following examples will show how to apply the Wagner–Kappus theory [5] specifically to open sections.

4.7. Secondary Warping

Up to now we have ignored the small contribution to axial warping occurring across the wall thickness. This is acceptable for most open sections but not for L- and T-sections where $\Gamma_1 = 0$ with their respective shear centres lying at the intersection between the rectangular limbs. These sections employ a secondary warping constant Γ_2 due to twist in the Wagner-Kappus theory. To derive Γ_2, generally, the contributions to the torque from both τ_{sz} and τ_{nz} in **Figure 6(b)** are required. That is, for components τ_{zs} and τ_{zn} acting within an elemental area $\delta s \times \delta n$ of the wall thickness shown in **Figure 7(a)**:

$$\delta T = \tau_{sz}(\delta s \times \delta n)R_t - \tau_{nz}(\delta s \times \delta n)R_n \tag{36a}$$

Now from the equilibrium Equations ((27a), (27b)) the shear stresses for the $s - z$ and $n - z$ planes are,

$$\tau_{sz} = -(\partial\sigma_z/\partial z)\delta s \quad \text{and} \quad \tau_{nz} = -(\partial\sigma_z/\partial z)\delta n,$$

Substituting into Equation (36a) and integrating for the limiting δT as $\delta s \to 0$ and $\delta n \to 0$:

$$\mathrm{d}T = -(\mathrm{d}s \times \mathrm{d}n)R_t\int_0^s(\partial\sigma_z/\partial z)\mathrm{d}s + (\mathrm{d}s \times \mathrm{d}n)R_n\int_0^n(\partial\sigma_z/\partial z)\mathrm{d}n \tag{36b}$$

The sum of Equations ((23a), (23b)) gives the total warping displacement as $\delta z \to 0$

$$w = -2(\mathrm{d}\theta/\mathrm{d}z)(A_E + R_n n) \tag{37}$$

from which the axial stress and its derivative follow:

$$\sigma_z = E\,\partial w/\partial z = -2E\left(\partial^2\theta/\partial z^2\right)(A_E + R_n n) \tag{38a}$$

$$\partial\sigma_z/\partial z = -2E\left(\partial^3\theta/\partial z^3\right)(A_E + R_n n) \tag{38b}$$

Substituting Equations ((38a), (38b)) into Equation (36b)

$$\begin{aligned} \mathrm{d}T &= 2E\left(\partial^3\theta/\partial z^3\right)\left[\int_0^s \left(A_E + R_n n\right)\mathrm{d}s \times \left(\mathrm{d}s \times \mathrm{d}n\right) R_t\right] \\ &- 2E\left(\partial^3\theta/\partial z^3\right)\left[\int_0^n \left(A_E + R_n n\right)\mathrm{d}n \times \left(\mathrm{d}s \times \mathrm{d}n\right) R_n\right] \end{aligned} \tag{39a}$$

Integrating (Equation (39a)) for T

$$\begin{aligned} T &= 2E\left(\partial^3\theta/\partial z^3\right)\int_0^n\left[\int_0^s\int_0^s \left(A_E + R_n n\right)\mathrm{d}s \times \left(R_t \times \mathrm{d}s\right)\right]\mathrm{d}n \\ &- 2E\left(\partial^3\theta/\partial z^3\right)\int_0^s\int_0^n\int_0^n \left(A_E + R_n n\right)\mathrm{d}n \times \left(R_n \times \mathrm{d}n\right)\Big]\mathrm{d}s \end{aligned} \tag{39b}$$

Noting from Equations (29c, d) that the first integral is negative, enables the total (Wagner) torque, arising from primary and secondary warping, to be written as a sum:

$$T = -E\left(\Gamma_1 + \Gamma_2\right)\left(\partial^3\theta/\partial z^3\right) = -E\Gamma_E\left(\partial^3\theta/\partial z^3\right) \tag{39c}$$

where, correspondingly, the *total warping constant* Γ_E is the sum of the primary and secondary warping constants, Γ_1 and Γ_2, appearing as the respective integrals [10]:

$$\Gamma_1 = 2\int_0^n\int_0^s\int_0^s \left(A_E + R_n n\right)\mathrm{d}s \times \left(R_t \times \mathrm{d}s\right)\Big]\mathrm{d}n \tag{40a}$$

$$\Gamma_2 = 2\int_0^s\int_0^n\int_0^n \left(A_E + R_n n\right)\mathrm{d}n \times \left(R_n \times \mathrm{d}n\right)\Big]\mathrm{d}s \tag{40b}$$

Integrating Equation (40a) by parts between limits 0 to s and n from $-t/2$ to $t/2$ again leads to Equation (29c). Equation (40b) integrates as a sum between similar limits:

$$\Gamma_2 = 2\int_0^s\left[\int_{-t/2}^{t/2}\int_0^n \left(A_E\mathrm{d}n\right) \times \left(R_n \times \mathrm{d}n\right)\right]\mathrm{d}s + 2\int_0^s\left[\int_{-t/2}^{t/2}\int_0^n \left(R_n n\mathrm{d}n\right) \times \left(R_n \times \mathrm{d}n\right)\right]\mathrm{d}s$$

$$\Gamma_2 = 2\int_0^s\left(\int_{-t/2}^{t/2} A_E R_n n\mathrm{d}n\right)\mathrm{d}s + \int_0^s\left(\int_{-t/2}^{t/2} R_n^2 n^2\mathrm{d}n\right)\mathrm{d}s$$

where the first integral is zero between the given limits of t. This leaves the second integral to define the *secondary warping constant* as

$$\Gamma_2 = \left(1/12\right)\int_0^s R_n^2 t^3\mathrm{d}s \tag{40c}$$

Hence the total warping constant $\Gamma_E = \Gamma_1 + \Gamma_2$ for *any* thin-walled open section becomes

$$\Gamma_E = \int_0^s \left(2A_E\right)^2\mathrm{d}s + \left(1/12\right)\int_0^s R_n^2 t^3\mathrm{d}s \tag{41}$$

4.8. Warping Constants

It has been shown how to evaluate the first integral Γ_1 due to bending. The secondary warping constant Γ_2 due to twist is usually small enough to be ignored but must be employed for sections where $\Gamma_1 = 0$, [16]. This is especially important in thicker sections where secondary warping stress due to twist can become significant, as the following examples show. For section **Figure 12(a)**, when s moves vertically with s along the mid-wall line from the outer edge D to E no area is subtended when the intersections between limbs coincides with the shear

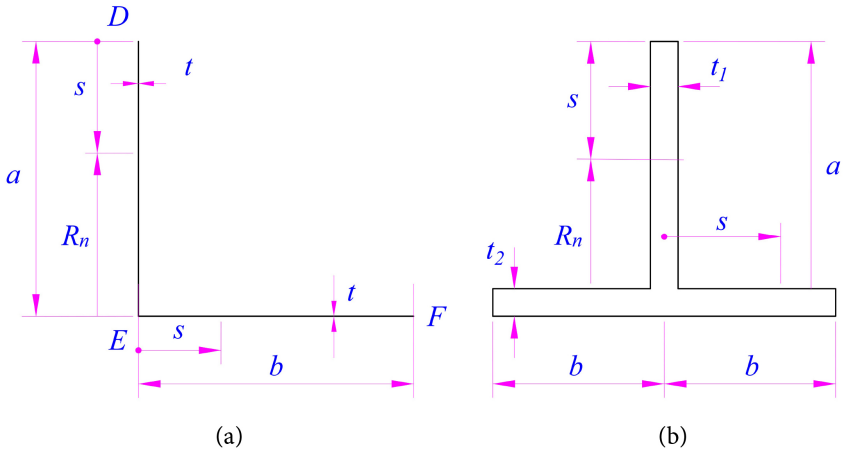

Figure 12. Thin angle sections with unequal limbs.

centre E. The same applies when s moves horizontally from E to F. Hence $\Gamma_1 = 0$ and so there is no primary warping in this section.

A similar result applies to Figure 12(b), *i.e.* for each angle section shown in Figure 12(a) and Figure 12(b), $\Gamma_1 = 0$. Hence secondary warping becomes the dominant (sole) mode. Therefore, expressions for the constants Γ_2 are required for the angle section geometries given in Figure 12(a) and Figure 12(b).

To determine Γ_2 from Equation (40c), R_n is measured within each limb with its centre at E. This gives $R_n = a - s$ for limb DE as shown and $R_n = s$ for limb EF. Then, given a constant thickness t for the angle section in Figure 12(a):

$$\begin{aligned}\Gamma_2 &= \left(t^3/12\right)\int_0^a (a-s)^2\,\mathrm{d}s + \left(t^3/12\right)\int_0^b s^2\mathrm{d}s \\ &= \left(t^3/12\right)\left\{\left[a^2 s - as^2 + s^3/3\right]_0^a + \left[s^3/3\right]_0^b\right\} \\ &= \left(t^3/36\right)\left(a^3 + b^3\right)\end{aligned}$$

Similar radii R_n apply to the inverted T-section, with different thicknesses t_1 and t_2 in Figure 12(b). A factor of 2 accounts for a flange length 2b bisected by the web.

$$\begin{aligned}\Gamma_2 &= \left(t_1^3/12\right)\int_0^a (a-s)^2\,\mathrm{d}s + \left(t_2^3/12\right)\int_0^b s^2\mathrm{d}s \\ &= \left(t_1^3/12\right)\left[a^2 s - as^2 + s^3/3\right]_0^a + \left(t_2^3/6\right)\left[s^3/3\right]_0^b \\ &= \left(t_1^3 a^3/36\right) + \left(t_2^3 b^3/18\right)\end{aligned}$$

5. Channel Section-Axial Torsion at Shear Centre

Stress calculations apply to seven points taken anticlockwise along the mean wall perimeter of the asymmetric channel (see Figure 13(a)): points 1 and 7 at the flange ends; points 3 and 5 at the corners; point 4 at the intersection with the x-axis and points 2 and 6 at the intersection with the y-axis. Consider a uniform thickness channel section cantilever beam with an axial torsion applied to the shear centre axis E. Firstly, it is required to determine the *primary warping constant* and the *unconstrained warping displacements*. These arise from opposing

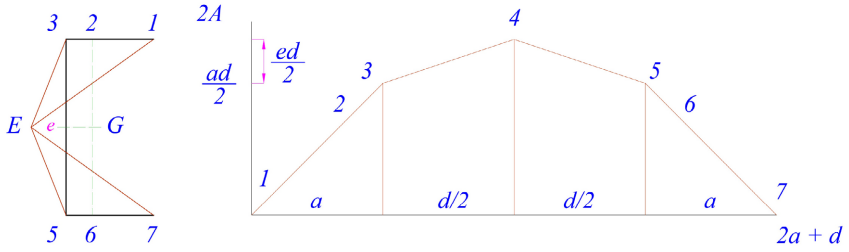

(a) (b)

Figure 13. Swept area for a channel section at the shear centre E.

torques T applied to the beam's free ends about a longitudinal axis passing through the shear centre E. For this analysis it is necessary to double the swept areas from E to points 1, 2, …, 7 for the ordinate of the plot shown in **Figure 13(a)** and **Figure 13(b)**.

The position of E has been found in the previous example as $e=3a^2/(d+6a)$, this allowing Equation (25c) to identify $\int y\mathrm{d}s$ with the enclosed area and $\int \mathrm{d}s$ as the perimeter length within **Figure 13(b)**. Applying the moment area theorem: $\breve{y}\int \mathrm{d}s=\int y\mathrm{d}s$ to **Figure 13(a)**, provides the centroid of the enclosed area:

$$(2a+d)\breve{y}=2\left[(d/2\times ed/2)+(d/2\times ed/2)+(d/4\times ed/2)\right]$$

Then

$$\breve{y}=(d/4)\left(2a^2+2ad+ed\right)/(2a+d)$$

When t is constant, the first integral $t\int y^2\mathrm{d}s$ in Equation (30b) requires equations of straight lines 1 - 2 - 3, 3 - 4, 4 - 5 and 5 - 6 - 7 for **Figure 13(b)**, as follows:

1 - 2 - 3 (limits/range $0\le s\le a$)

$$y=ds/2;\ \int y^2\mathrm{d}s=\int_0^a(ds/2)^2\,\mathrm{d}s=d^2a^3/12$$

3 - 4 [limits/range $a\le s\le (a+d/2)$]

$$y=es+(ad/2-ea);$$

$$\int y^2\mathrm{d}s=\int_a^{a+d/2}(es+ad/2-ea)^2\,\mathrm{d}s$$

$$=\int_a^{a+d/2}\left[e^2s^2+2es(ad/2-ea)+(ad/2-ea)^2\right]\mathrm{d}s$$

$$=(d^3/24e)\left[(a+e)^3-a^3\right]$$

4 - 5 [limits/range $(a+d/2)\le s\le (a+d)$]

$$y=-se+(ad/2+ed+ae);$$

$$\int y^2\mathrm{d}s=\left[-se+(ad/2+ae)\right]^2\mathrm{d}s=(d^3/24e)\left[(a+e)^3-a^3\right]$$

5 - 6 - 7 [limits/range $(a+d)\le s\le (2a+d)$]

$$y=-ds/2+d(a+d/2);\ \int y^2\mathrm{d}s=\int_{a+d}^{2a+d}\left[-ds/2+d(a+d/2)\right]^2\mathrm{d}s=d^2a^3/12$$

The primary warping constant Γ_1 is found from Equation (29) as follows:

$$\Gamma_1/t = 2\left\{d^2a^3/12 + \left(d^3/24e\right)\left[\left(a+e\right)^3 - a^3\right]\right\}$$
$$-\left(d^2/16\right)\left(2a^2 + 2ad + ed\right)^2 \Big/ \left(2a+d\right)$$

and the axial warping displacements w from Equation (23a):

$$w = -2A_E\left(\delta\theta/\delta z\right) = -\left(y - \breve{y}\right)T/GJ$$

This gives displacements at the corner, free-end and web centre positions:

$$\left(GJ/T\right)w_1 = \left(GJ/T\right)w_7 = \breve{y}$$
$$\left(GJ/T\right)w_3 = \left(GJ/T\right)w_5 = \breve{y} - ad/2$$
$$\left(GJ/T\right)w_4 = \breve{y} - d\left(a+e\right)/2$$

The analysis proceeds in relation to three US standard thin-walled channels, extruded to the following Imperial dimensions:

A) a = 1/2", d = 1", t = 1/16", L = 300 mm (11.81");

B) a = 1", d = 1¾", t = ⅛", L = 1 m (39.37");

C) a = 5/8", d = 1⅞", t = 3/64", L = 340 mm (13.39").

where a is the length of each horizontal flange, d is the depth of the vertical web, t is the uniform thickness and L is the beam length. To avoid unnecessary conversions of the Imperial units various ratios are adopted for the calculations that follow including each section's non-dimensional geometrical ratios given above.

5.1. Unconstrained Warping

The following *unconstrained* axial warping displacements w apply to points 1, 3, 4, 5 and 7. They appear in fractions of a^2 to allow conversion from the constants G, J and T:

Section A:

$$e/a = 3/8,\ X'/a = 1/4,\ \breve{y}/a^2 = 27/32$$
$$\left(GJ/T\right)w_1 = \left(GJ/T\right)w_7 = 27a^2/32$$
$$\left(GJ/T\right)w_3 = \left(GJ/T\right)w_5 = -5a^2/32$$
$$\left(GJ/T\right)w_4 = -17a^2/32$$

Section B:

$$e/a = 12/31,\ X'/a = 4/15,\ \breve{y}/a^2 = 0.7207$$
$$\left(GJ/T\right)w_1 = \left(GJ/T\right)w_7 = 0.7207a^2$$
$$\left(GJ/T\right)w_3 = \left(GJ/T\right)w_5 = -0.1543a^2$$
$$\left(GJ/T\right)w_4 = -0.493a^2$$

Section C:

$$e/a = 1/3,\ X'/a = 1/5,\ \breve{y}/a^2 = 27/20$$

$$(GJ/T)w_1 = (GJ/T)w_7 = 27a^2/20$$

$$(GJ/T)w_3 = (GJ/T)w_5 = -3a^2/20$$

$$(GJ/T)w_4 = -13a^2/20$$

which are distributed consistently over each section in the manner of Figure 14. Within this distribution, at the centroid axis intersections, point 2 lies upon the line 1 - 3 and point 6 lies upon the line 5 - 7, providing their axial displacements w proportionately.

These unconstrained displacements arise from equal, opposing "St Venant" torques T_v applied about a longitudinal axis through the shear centre in a given length L of each channel cross-section. The angular twist θ between the ends follows from the St Venant torque as: $\theta = T_vL/GJ$, where $J = (1/3)\Sigma bt^3$ for a thin-walled open section and G is the shear modulus. To apply these formulae, take, for example, section A subjected to a torque $T_v = 10$ Nm. The warping displacement at position 1 is calculated from the expressions given above as follows:

$$J = (1/3)\sum bt^3/3 = (2a+d)t^3/3 = 4at^3/3 = 4\times 12.7\times(25.4/16) = 67.74 \text{ mm}^4$$

$$(GJ/T)w_1 = 27a^2/32$$

$$\therefore w_1 = 27/32\times a^2T/GJ$$

$$= 27/32\times 12.7^2\times\left(10\times 10^3\right)\Big/\left(70\times 10^3\times 67.74\right) = 0.287 \text{ mm}$$

The angular twist expression gives

$$\theta = T_vL/GJ = \left(10\times 10^3\times 300\right)\Big/\left(70\times 10^3\times 67.74\right) = 0.633 \text{ rad} = 36.25^\circ$$

5.2. Constrained Torsion

Warping displacements w are constrained when one end section is fixed and the torque T is applied about the axis through E at the opposite free end. At the fixing, because w is completely constrained, axial stress σ_z arises. At the free end and within the length $0 < z \le L$, a partial constraint applies to which Equations (35b) apply. In calculating torsional stiffness and axial stress for the three sections with dimensions A, B and C given above, the following constants and ratios apply.

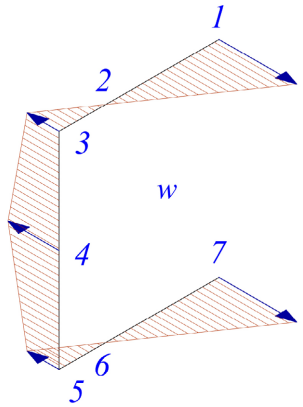

Figure 14. Unconstrained axial warping displacement distribution.

Section A: $a = 1/2"$, $d = 1"$, $t = 1/16"$, $L = 300$ mm (11.81")

$t/a = 1/8$, $L/a = 23.62$, $d/a = 2$, $e/a = 3/8$, $\breve{y} = 27a^2/32$

1) ***Constants***

$$\Gamma_1/(a^5 t) = 2(1/3) + (1/12)2^3(8/3)\left[(11/8)^3 - 1\right] - 2^2\left[2(1+2) + (3/8\times 2)\right]^2 / \left[16(2+2)\right]$$

$$= 0.667 + 2.844 - 2.848 = 0.6628$$

$$\Gamma_1 = 0.6628a^5 t = 524.48\times 10^3 \text{ mm}^6$$

$$J = (t^3/3)(2a+d) = (4/3)at^3 = (4/3)\times 12.7\times(25.4/16)^3 = 67.74 \text{ mm}^4$$

$$E/G = 210/70 = 3$$

$$\mu = \sqrt{GJ/E\Gamma_1} = \sqrt{4at^3/(9\times 0.6628a^5 t)} = 0.8189t/a^2$$

$$\mu L = 0.8189(t/a)(L/a) = 0.8189\times 0.125\times 300/12.7 = 2.4179$$

$$\exp(-2\mu L) = \exp(-4.836) = 7.938\times 10^{-3}$$

2) ***From Equation (32b) the constrained, free-end torsional stiffness* is:**

$$T/G\theta = \left[\mu J\left(1+\exp(-2\mu L)\right)\right] / \left[(\mu L - 1) + (\mu L + 1)\exp(-2\mu L)\right]$$

$$= 0.8189t/a^2 \times 4at^3/3 \times 0.6975$$

$$\therefore T/\theta = 70\times 10^3 \times 0.7616t^4/a = 26.67\times 10^3 \text{ N}\cdot\text{mm/rad}$$

$$= 26.67 \text{ N}\cdot\text{m/rad}$$

to be compared with an *unconstrained St Venant's stiffness*:

$$T_v/\theta = GJ/L = 70\times 10^3 \times 67.74/300 = 15.806 \text{ N}\cdot\text{m/rad}$$

In which the 50 % increase in T/θ is due to the Wagner-Kappus contribution to the increased stiffness.

3) ***The fixed-end axial stress distribution for z = 0 follows from Equations (26) and (34a) as***

$$\sigma_z = -\left[(y-\breve{y})T/(\mu\Gamma_1)\right]\times\left(1-\exp(-2\mu L)\right)/\left(1+\exp(-2\mu L)\right)$$

$$= \left[(y-\breve{y})T/\left(0.8188t/a^2\times 0.6628a^5 t\right)\right]\times 0.9842$$

$$= 1.8135T(\breve{y}-y)/a^3t^2$$

$$a^3t^2\sigma_z/T = 1.8135(\breve{y}-y)$$

and referring to Figure 13(a) for y at end and corner positions 1 and 3 and at the web centre 4:

$y_1 = 0$, then $a^3t^2(\sigma_z)_1/T = 1.8135\breve{y} = 1.8135\times 27a^2/32 = 1.53a^2$

$$(\sigma_z)_1 = 1.53at^2 = (\sigma_z)_7$$

$y_3 = ad/2$, then

$$a^3t^2(\sigma_z)_3/T = 1.8135(\breve{y} - ad/2)$$

$$= 1.8135(27/32 - 1)a^2 = -0.2834a^2$$

$$(\sigma_z)_3 = -0.2834T/at^2 = (\sigma_z)_5$$

$y_4 = (a+e)d/2$, then, $a^3t^2(\sigma_z)_4/T = 1.8135(\bar{y} - ad/2 - ed/2)$

$$= 1.8135(27/32 - 1 - 0.375)a^2 = -0.9634a^2$$

$$(\sigma_z)_4 = -0.9634T/at^2$$

Section B: a = 1", d = 1¾", t = ⅛", L = 1 m (39.37")

t/a = 1/8, L/a = 39.37, d/a = 1¾, e/a = 12/31, $\bar{y} = 0.7207a^2$

1) Constants

$$\Gamma_1/(a^5t) = (1/6)(7/4)^2 + (1/12)(7/4)^3(31/12)\left[(1+12/31)^3 - 1\right]$$

$$-(7/4)^2\left[2(1+7/4) + (12/31)(7/4)\right]^2/\left[16(2+7/4)\right]$$

$$= 0.5104 + 1.9254 - 1.9478 = 0.488$$

$$\Gamma_1 = 0.488a^5t = 16.381\times10^6 \text{ mm}^6$$

$$J = (t^3/3)(2a+d) = (5/4)at^3 = 1016.8 \text{ mm}^4$$

$$E/G = 210/70 = 3$$

$$\mu = \sqrt{GJ/E\Gamma_1} = \sqrt{5at^3/(4\times3\times0.488a^5t)} = 0.924t/a^2$$

$$\mu L = 0.924(t/a)(L/a) = 0.924\times39.37/8 = 4.547$$

$$\exp(-2\mu L) = \exp(-9.095) = 0.112\times10^{-3}$$

2) The Torsional Stiffness follows from the free-end angular twist as:

$$T/G\theta = \left[\mu J(1+\exp(-2\mu L))\right]/\left[(\mu L - 1) + (\mu L + 1)\exp(-2\mu L)\right]$$

$$= 0.924t/a^2 \times 5at^3/4 \times 0.2819$$

$$\therefore T/\theta = 70\times10\times0.3256t^4/a = 91.18\times10^3 \text{ N}\cdot\text{mm/rad} = 91.18 \text{ N}\cdot\text{m/rad}$$

Here with the increased beam length of 1 m for section B) the torsional stiffness this channel section agrees with its asymptotic value:

$$T/\theta \to \mu GJ/(\mu L - 1) = 4.55\times10^{-3}\times70\times10^3\times1016.8/(4.55-1)$$

$$= 91.23 \text{ N}\cdot\text{m/rad}$$

to be compared with the St Venant's torsional stiffness for when both ends are free:

$$T_v/\theta \to GJ/L = 70\times10^3\times1016.8/1000 = 71.18 \text{ N}\cdot\text{m/rad}$$

which for section B) lies at its closest for to the stiffness (91.18 Nm/rad) in a 1 m long thin-walled channel beam with one end constrained.

3) At the fixed end ($z = 0$) axial stress distribution follows from Equation (34a), in which the corresponding near asymptotic values apply

$$\sigma_z = -\left[(y-\bar{y})T/(\mu\Gamma_1)\right]\times(1-\exp(-2\mu L))/(1+\exp(-2\mu L))$$

$$\approx 2(y-\bar{y})T/(\mu\Gamma_1)$$

$$= -\left[(y-\bar{y})T/(0.924t/a^2)\times0.488a^5t\right]\times0.99977$$

$$= -2.217T(y-\bar{y})/a^3t^2$$

$$a^3t^2\sigma_z/T = 2.217\left(\breve{y}-y\right)$$

and referring to Figure 13(a) and Figure 13(b) for y at each position 1 and 3 and at the web centre 4:

$$y_1 = 0\text{, then}\quad a^3t^2\left(\sigma_z\right)_1/T = 2.217\breve{y} = 2.217\times 0.7207a^2 = 1.5978a^2$$

$$\left(\sigma_z\right)_1 = 1.5978T/at^2 = \left(\sigma_z\right)_7$$

$$y_3 = ad/2\text{, then}\quad \begin{aligned} a^3t^2\left(\sigma_z\right)_3/T &= 2.217\left(\breve{y}-ad/2\right)\\ &= 2.217\left(0.7207-7/8\right)a^2 = -0.3421a^2\end{aligned}$$

$$\left(\sigma_z\right)_3 = -0.3421T/at^2 = \left(\sigma_z\right)_5$$

$$y_4 = \left(a+e\right)d/2\text{, then,}\quad \begin{aligned} a^3t^2\left(\sigma_z\right)_4/T &= 2.217\left(\breve{y}-ad/2-ed/2\right)\\ &= 2.217\left[0.7207-7/8-\left(7/8\right)\left(12/31\right)\right]a^2 = -1.093a^2\end{aligned}$$

$$\left(\sigma_z\right)_4 = -1.093T/at^2$$

Section C: a = 5/8", d = 1⅞", t = 3/64", L = 340 mm (13.39")

t/a = 3/40, L/a = 22, d/a = 3, e/a = 1/3, $\breve{y} = 27a^2/20$

1) ***Constants***

$$\begin{aligned}\Gamma_1/\left(a^5t\right) &= \left(1/6\right)\left(9/6\right)+\left(1/12\right)\left(3^3\times 3\right)\left[\left(4/3\right)^3-1\right]\\ &\quad -3^2\left[2\left(1+3\right)+\left(1/3\times 3\right)\right]^2/\left[16\left(2+3\right)\right]\\ &= 1.5+9.25-9.1125 = 1.6375\end{aligned}$$

$$\Gamma_1 = 1.6375a^5t = 1.966\times 10^6\ \text{mm}^6$$

$$J = \left(t^3/3\right)\left(2a+d\right) = \left(5/3\right)at^3 = 44.656\ \text{mm}^4$$

$$E/G = 210/70 = 3$$

$$\mu = \sqrt{GJ/E\Gamma_1} = \sqrt{5at^3/\left(9\times 1.6375a^5t\right)} = 0.5825t/a^2$$

$$\mu L = 0.5825\left(t/a\right)\left(L/a\right) = 0.5825\times\left(3/40\right)\times 22 = 0.9611$$

$$\exp\left(-2\mu L\right) = \exp\left(-1.922\right) = 0.1462$$

2) Equation (32b) provides the constrained, torsional stiffness [4] ***at free-end as:***

$$\begin{aligned}T/G\theta &= \left[\mu J\left(1+\exp\left(-2\mu L\right)\right)\right]/\left[\left(\mu L-1\right)+\left(\mu L+1\right)\exp\left(-2\mu L\right)\right]\\ &= \left(0.5825t/a^2\right)\left(5/3\right)at^3\times 4.6252 = 4.4904t^4/a\end{aligned}$$

$$\begin{aligned}\therefore T/\theta &= 4.4904\times 70\times 10^3\times 1.1906^4/15.875\\ &= 39.79\times 10^3\ \text{N}\cdot\text{mm/rad} = 39.79\ \text{N}\cdot\text{m/rad}\end{aligned}$$

to be compared with an unconstrained St Venant's torsional stiffness [5]:

$$T_v/\theta = GJ/L = 70\times 10^3\times 44.656/340 = 9.194\ \text{N}\cdot\text{m/rad}$$

For channel section C), a greater than fourfold increase in its constrained stiffness is attributed to the Wagner-Kappus contribution to the total torque.

3) The fixed end (z = 0) axial stress distribution follows from Equation (34a) as

$$\sigma_z = -\left[\left(y-\breve{y}\right)T/\left(\mu\Gamma_1\right)\right]\times\left(1-\exp\left(-2\mu L\right)\right)/\left(1+\exp\left(-2\mu L\right)\right)$$

$$\sigma_z = -\left[\left(y-\breve{y}\right)T/\left(0.5825t/a^2\times 1.6375a^2t\right)\right]\times\left(1-0.1462\right)/\left(1+0.1462\right)$$

$$= 0.7809T\left(y-\breve{y}\right)/a^3t^2$$

$$a^3t^2\sigma_z/T = 0.7809\left(\breve{y}-y\right)$$

Referring this equation to Figure 13(a) and Figure 13(b), for *y* at each position 1, 3 and 4:

$y_1 = 0$, then $a^3t^2\left(\sigma_z\right)_1/T = 0.7809\breve{y} = 0.7809\times 27a^2/20 = 1.054a^2$

$$\left(\sigma_z\right)_1 = 1.054T/at^2 = \left(\sigma_z\right)_7$$

$y_3 = ad/2$, then $a^3t^2\left(\sigma_z\right)_3/T = 0.7809\left(\breve{y}-ad/2\right) = 0.7809\left(27/20-1.5\right)a^2 = -0.1171a^2$

$$\left(\sigma_z\right)_3 = -0.1171T/at^2 = \left(\sigma_z\right)_5$$

$y_4 = \left(a+e\right)d/2$, then, $a^3t^2\left(\sigma_z\right)_4/T = 0.7809\left(\breve{y}-ad/2-ed/2\right) = 0.7809\left(27/20-1.5-0.5\right)a^2 = -0.5076a^2$

$$\left(\sigma_z\right)_4 = -0.5076T/at^2$$

5.3. Axial Stress Distribution

Figure 15 shows the common manner in which the axial stress in each section is distributed across its fixed end. The greatest axial tensile stress occurs at the flange ends (points 1 and 7) and the greatest compressive stress lies at the web's mid-position 4.

The normalised axial stress calculated at each position 1, 3 and 4 per unit torque are listed for the three channel geometries in Table 1. Referring to Figure 15, there is an equality in stress between flange end positions 1 and 7 and between corner positions 3 and 5 as shown.

The entries given in Table 1 along with the section dimensions ($a \times t$) allow a calculation of the stress magnitudes that apply to Figure 15. Taken with the conversion of each section's Imperial dimensions ($a \times t$) each entry allows a calculation of the stress magnitude. For example, if a "unit" torque of 1 Nm is applied across the top row then the normalised stress entries at position 1 for channel sections A, B and C are converted to axial stress in MPa as follows:

Table 1. Normalised axial stress $(at^2/T)\sigma_z$ at positions 1, 3 and 4 for three channel cross-sections with torque at E.

Section ($a \times t$) →	(a) ½" × 1/16"	(b) 1" × ⅛"	(c) 5/8" × 3/64"
1	1.53	1.5978	1.054

3	−0.2834	−0.3421	−0.1171
4	−0.9634	−1.093	−0.5076

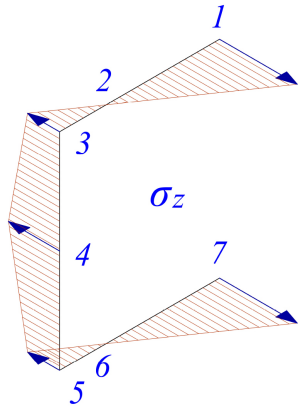

Figure 15. Axial stress distribution at the channel fixing with axial torque applied to an axis through the shear centre.

$$\sigma_z = 1.530T/at^2 = 1.530\times\left(1\times10^3\right)\Big/\left[\frac{1}{2}\times\frac{1}{16^2}\times25.4^3\right] = 47.80\text{ MPa}$$

$$\sigma_z = 1.5978T/at^2 = 1.5978\times\left(1\times10^3\right)\Big/\left[1\times\frac{1}{8^2}\times25.4^3\right] = 6.24\text{ MPa}$$

$$\sigma_z = 1.004T/at^2 = 1.004\times\left(1\times10^3\right)\Big/\left[\frac{5}{8}\times\left(\frac{3}{64}\right)^2\times25.4^3\right] = 44.61\text{ MPa}$$

Under this torque value such elastic stress magnitudes may be borne by an aluminium beam at the end fixing without yielding occurring, given that they diminish to zero at the free end.

Finally, in answer to the question: What is the relationship between axial stress and constrained warping? Equation (34c) shows that there is no axial stress at the free end ($z = L$) where the maximum warping displacement occurs. The influence of constraining warping at the fixed end extends to all intermediate sections in the beam length where, for $0 < z < L$, Equations (34c) and (35b) provide the interdependent relationship between warping displacement and stress. At the fixed-end of a cantilevered beam, where $z = 0$, these equations show that $w = 0$ with $\sigma_z = \mu E w_o \tanh(\mu L)$ at its maximum. At the free end where $z = L$, then $\sigma_z = 0$ and the warping displacement $w = w_o(1 - 1/\cosh\mu L)$ takes its maximum value, this being less than the "free" warping displacement w_o where.

$$w_o = -2A_E\left(\delta\theta/\delta z\right) = -\left(y - \bar{y}\right)T/GJ \tag{42a}$$

For all other "constant" position $0 < z < L$ in the length Equation (34b) has shown that σ_z is proportional to w_o in which the constant of proportionality is identified as:

$$\sigma_z = \mu E\left\{\sinh\left[\mu\left(L - z\right)\right]/\cosh\left(\mu L\right)\right\}\times w_o \tag{42b}$$

Combining Equations ((42a), (42b)) then shows how σ_z varies with the sec-

tion's swept area A_E at a given position in the length:

$$\sigma_z = \mu E\left\{\sinh\left[\mu\left(L-z\right)\right]/\cosh\left(\mu L\right)\right\}\times\left(y-\breve{y}\right)T/GJ$$

$$\sigma_z = \mu ET/GJ\left\{\sinh\left[\mu\left(L-z\right)\right]/\cosh\left(\mu L\right)\right\}\times\left(y-\breve{y}\right)$$

$$\sigma_z = \left(2T/\mu\Gamma_1\right)\left\{\sinh\left[\mu\left(L-z\right)\right]/\cosh\left(\mu L\right)\right\}\times A_E \quad (42c)$$

Equation (42c) shows that the axial stress depends upon the constrained warping displacement distribution in the cross-section at a given position in the length

6. Conclusions

Thin-walled cantilever beam of open channel section will bend and twist when its free end transverse loading is applied at the section's centroid. Twist is eliminated when that loading is displaced to the shear centre. A reciprocal behaviour is found when a torque is applied about a longitudinal axis through the centre of twist where torsion is not accompanied by bending. However, this torsion is not pure for a cantilever beam when its one fixed-end constrains completely the natural warping that would be found when both ends are free. In this paper the two "centres" have been assumed to coincide.

A theoretical basis for coincidence has examined the influence of an applied torque displaced from the shear centre E to the centroid G and to the web centre O. There it is found that an unconstrained warping distribution and the constrained axial stress distribution depend in a similar manner upon the axis of torsion. Differences between these two distributions for axes at E and G and between axes at E and O would suggest that a coincidence between centres is a valid assumption to be adopted here, however, having a combined torsion and bending loads applied to a thin walled-structure will result of different behaviour, and for the extended analyses given in [17].

Conflicts of Interest

The authors David Rees, and Abdelraouf Alsheikh, have received research support from the Department of Design. The authors declare that they have no conflict of interest.

References

[1] Vlasov, V.Z. (1961) Thin-walled Elastic Beams. Oldbourne Press, London.

[2] Al-Sheikh, A.M.S. and Rees, D.W.A. (2021) General Stiffness Matrix for a Thin-Walled, Open-Section Beam Structure. *World Journal of Mechanics*, **11**, 205-236. https://doi.org/10.4236/wjm.2021.1111015

[3] Al-Sheikh, A.M.S. and Rees, D.W.A. (2022) Transformation Matrix for Combined Loads Applied to Thin-Walled Structures. *World Journal of Mechanics*, **12**, 65-78. https://doi.org/10.4236/wjm.2022.126006

[4] Boresi, A.P., Schmidt, R.J. and Sidebottom, O.M. (1993) Advanced Mechanics of

Materials. J. Wiley and Son, New York.

[5] Wagner, H. (1936) National Advisory Committee for Aeronautics, Technical Memorandum No. 807. https://ntrs.nasa.gov/api/citations/19930094608/downloads/19930094608.pdf

[6] Rees, D.W.A. (2015) The Mechanics of Engineering Structures. IC Press, London.

[7] Rees, D.W.A. (2016) Mechanics of Solids and Structures. 2nd Edition, IC Press, London.

[8] Rees, D.W.A. and Al-Sheikh, A.M.S. (2024) The Longitudinal Axis of Loading Thin-Walled Beams of Open Section. Part II. *World Jl Mech*. (in press)

[9] Gjelsvik, A. (1981) The Theory of Thin-Walled Beams. Wiley, Hoboken.

[10] Bleich, F and Bleich, H.H. (1952) Buckling Strength of Metal Structures, McGraw-Hill, New York.

[11] Hoff, N.J. (1943) *Article Title. Jl Roy Aero Soc.*, **87**, 35-83.

[12] Williams, D. (1960) Theory of Aircraft Structures. E. Arnold, London.

[13] Oden, J.T. and Ripperger, E.A. (1980) Mechanics of Elastic Structures. 2nd Edition, McGraw-Hill, New York.

[14] Wang, G. (2012) Restrained Torsion of Open Thin-Walled Beams Including Shear Deformation Effects. *Journal of Zhejiang University Science A*, **13**, 260-273. https://doi.org/10.1631/jzus.A1100149

[15] Bhatt, P. and Nelson, H.M. (1990) Structures. 3rd Edition, Longman, London.

[16] Megson, T.H.G. (1972) Aircraft Structures for Engineering Students. E. Arnold, London.

[17] Al-Sheikh, A.M.S. (1985) Behaviour of Thin-Walled Structures under Combined Loads. Ph. D. Thesis, Loughborough University of Technology, Loughborough, UK.

List of Symbols

a, d, t	cross-section dimensions
A	cross-sectional area
e_x, e_y	shear centre position
X'	centroid position
x, y	centroid co-ordinates
D_x, D_y	first moments of area
E	tensile modulus
F_x, F_y	transverse shear forces
G	shear modulus
I_x, I_y	second moments of area
J	St Venant's torsion constant
L	beam length
M_x, M_y	bending moments
N	wall normal
q	shear flow
R	perpendicular length
s	wall median co-ordinate
t	wall thickness
T	axial torque
u, v	principal co-ordinate axes
w	constrained warping displacement
w_o	unconstrained warping displacement
y	swept area ordinate = $2A_E$
$\bar{y}$	swept area mean
z	length co-ordinate
ε_z,	axial strain
Γ_1	primary warping constant
μ	warping constant
σ_z	axial stress
τ_{zs}	shear stress
θ	angular twist